CONTROL-THEORY AND ADVANCED TECHNOLOGY
Vol. 10, No. 4, Part 4, pp. 1563–1590, November, 1995

C93130R

Contributed Paper

ENERGY FLOW CONTROL OF INTERCONNECTED STRUCTURES: I. MODAL SUBSYSTEMS*

Y. KISHIMOTO,[1] D. S. BERNSTEIN[2] AND S. R. HALL[3]

Abstract. Dissipative energy flow controllers are designed for interconnected modal subsystems. Active feedback controllers for vibration suppression are then viewed as either an additional subsystem or a dissipative coupling. These controllers, which are designed by the LQG positive real control approach, maximize energy flow from a specified modal subsystem.

Key Words—Energy flow, control of flexible structures.

1. Introduction

Energy flow has been widely studied as an effective tool for analyzing large, interconnected vibrating systems (Bernstein and Hyland, 1991; Crandall and Lotz, 1971; Davies, 1972 a; b; 1973; Langley, 1992; Lyon, 1975; Lyon and Maidanik, 1962; Mace, 1992 a; b; Maidanik, 1981; Miller and Von Flotow, 1989; Newland, 1968; Norton, 1989; Pan et al., 1992; Pinnington and White, 1981; Smith, Jr., 1979; Von Flotow, 1986; Woodhouse, 1981). One of the key results of this approach is the fact that, within interconnected subsystems, energy flow can often be expressed as a linear combination of subsystem energy.

Energy flow modeling techniques can be categorized into two groups, namely, the wave propagation approach (Langley, 1992; Mace, 1992 a; b; Miller and Von Flotow, 1989; Pinnington and White, 1981; Von Flotow, 1986) and the modal approach (Crandall and Lotz, 1971; Davies, 1972 a; b; 1973; Lyon, 1975; Lyon and Maidanik, 1962; Maidanik, 1981; Newland, 1968; Pan et al., 1992; Smith, Jr., 1979; Woodhouse, 1981). For the wave propagation approach, Von Flotow (1986) and Miller and Von Flotow (1989) analyzed structural networks, while Mace (1992 b) calculated the energy flow between two interconnected beams. The wave approach can also be applied to irregular structures MacMartin and Hall (1991) by using concepts from structural acoustics (Lyon, 1987). Using the modal approach, the energy flow between two interconnected

* Received by the editors November 1, 1993 and in revised form November 14, 1994.
This research was supported in part by the Air Force Office of Scientific Research under Grant F49620-92-J-0127 and the NASA SERC Grant NAGW-1335.
[1] Kougi-Tai Hijitsu-Gun, Gifu Air Base, Mubanchi Naka Kanyuchi, Gifu 504, Japan.
[2] Department of Aerospace Engineering, The University of Michigan, Ann Arbor, MI 48109-2118, U.S.A.
[3] Department of Aeronautics and Astronautics, Massachusetts Institute of Technology, Cambridge, MA 02139, U.S.A.

beams was calculated in Crandall and Lotz (1971) and Davies (1972 a; b; 1973), while energy flow between a rigid body and the supporting panel was studied by Pan et al. (1992). Furthermore, Statistical Energy Analysis (SEA), based on both approaches, has been extensively developed and successfully applied to practical problems in vibrations and acoustics (Lyon, 1975; Lyon and Maidanik, 1962; Maidanik, 1981; Newland, 1968; Smith, Jr., 1979; Woodhouse, 1981).

In active feedback control for reducing vibration, energy flow has been considered as a performance index to be minimized (Mace, 1987; MacMartin and Hall, 1991; 1994; Miller et al., 1990; Pan and Hansen, 1991; Von Flotow and Shäfer, 1986). The design of these active controllers, however, has proven to be a challenging problem. For example, the optimal controller is often noncausal (MacMartin and Hall, 1991) and thus asymptotic stability of the closed-loop system cannot be guaranteed. Furthermore, active energy flow control for interconnected structures composed of more than two subsystems has received limited attention due to the lack of energy flow models for such interconnected systems.

In recent work (Kishimoto and Bernstein, 1995 a; b; Kishimoto et al., 1995 a) motivated by Wyatt et al. (1984), deterministic energy flow model was derived for a structure consisting of several modal subsystems that are coupled either conservatively or dissipatively. In the present paper, our goal is to apply the results of Kishimoto and Bernstein (1995 a; b) and Kishimoto et al. (1995 a) to design active control laws for coupled structures. For this purpose, we design active control laws for modal subsystems in this paper, while structural subsystems are considered in a companion paper (Kishimoto et al., 1995 b).

Three typical situations requiring energy flow controllers are considered in this paper. First, in Sec. 4, we consider energy flow control for several subsystems interconnected by conservative coupling (Kishimoto and Bernstein, 1995 a). For such an interconnected system, the control law is designed for the system as a whole by means of an energy flow model for the entire system including the controller. We thus treat the feedback controller as an additional subsystem interconnected by a conservative coupling, so that energy flow is controlled through the coupling.

Next, in Sec. 5, we consider energy flow control among individual structural modes. Here we exploit the fact that structural modes are essentially coupled by the input and output matrices. By enlarging the input and output matrices, we design a dissipative feedback controller that serves, in effect, as a dissipative coupling (Kishimoto and Bernstein, 1995 b). As an application of this approach, in Sec. 6 we consider two uncoupled systems that are controlled by a relative force actuator.

In both cases, the controller is designed to maximize the steady state energy flow from one of the subsystems in order to reduce the vibration of a specified subsystem. The control approach we use is due to Lozano-Leal and Joshi (1990), with refinements by Haddad et al. (1994). This approach is briefly reviewed in Sec. 3. Since the controller and plant are both positive real, closed-loop asymptotic stability is guaranteed in spite of modeling uncertainty.

Notation.

$\mathscr{E}$: expectation

S_{xx}: power spectral density matrix of x

S_{xy}: cross spectral density matrix of x and y
I: identity matrix
j: $\sqrt{-1}$
$A_{(k,l)}$: (k, l)-element of A
$\mathrm{Re}[A]$, $\mathrm{Im}[A]$: real, imaginary part of A
$\mathrm{diag}(a_1, \cdots, a_r)$: diagonal matrix whose ith diagonal element is a_i
A^T, A^*: transpose, complex conjugate transpose of A
$A > (\geq) 0$: symmetric positive (nonnegative) definite matrix
e_i: ith column of I
$\mathrm{tr}[A]$: trace of A
$G(s) \sim \left[\begin{array}{c|c} A & B \\ \hline C & D \end{array}\right]$: state space realization of the transfer function $G(s) = C(sI - A)^{-1}B + D$
B_0: diagonal matrix generating modal subsystem
$\tilde{B}$: column vector generating relative force and velocity
c_i: resistance or damping of ith subsystem
D: disturbance matrix
E_1, E_2: measurement matrices for LQG performance index
k_i: stiffness of ith subsystem
$L(s)$: linear time-invariant coupling matrix
m_i: mass of ith subsystem
P, Q: solutions of LQG Riccati equations
P_i^c: steady-state average coupling energy flow of ith subsystem
P_i^d: steady-state average energy dissipation rate of ith subsystem
P_i^e: steady-state average external energy flow of ith subsystem
Q_0: positive-definite matrix for strictly positive real plant
$\tilde{Q}$: steady-state covariance for feedback representation of interconnected system
$q_i(t)$: modal coordinate of ith mode
R_1, R_2, V_1, V_2: weighting matrices for LQG controller
$\tilde{w}_i(t)$: normalized unit intensity white noise disturbance
$Z(s)$: subsystem impedance matrix
$z_i(s)$: subsystem (impedance transfer function)
ζ_i: structural damping coefficient
$\chi(\xi, t)$: modal decomposition
ξ: structural coordinate
ξ_i: location of the ith actuator
ξ_i: location of the ith disturbance
ρ: mass density
$\psi_i(\xi)$: eigenfunction of ith mode
ω_i: natural frequency of ith mode

2. Energy Flow Model for Interconnected Systems

In this section, we briefly review some results concerning energy flow obtained in Kishimoto and Bernstein (1995 a; b) and Kishimoto et al. (1995 a). Consider r subsystems $z_1(s), \cdots, z_r(s)$ interconnected by a linear time-invariant coupling $L(s)$. An electrical representation of this interconnection involving scalar impedances $z_i(s)$ is given in Fig. 1 which is adapted from Kishimoto and Bernstein (1995 a; b), Kishimoto et al. (1995 a) and Wyatt et al. (1984). Each subsystem $z_i(s)$ is assumed to be a strictly positive real and thus asymptotically stable scalar transfer function. We assume that the disturbance vector $w_0(t) \triangleq [w_1(t) \cdots w_r(t)]^T$ is given by

$$w_0(t) = D\tilde{w}(t), \tag{1}$$

where $D \in \mathscr{R}^{r\times d}$ is a constant matrix and $\tilde{w}(t) \triangleq [\tilde{w}_1(t) \cdots \tilde{w}_d(t)]^T$ is normalized white noise whose intensity matrix is identity. Thus the intensity matrix $S_{w_0w_0}$ of $w_0(t)$ is given by $S_{w_0w_0} = DD^T$. Now we denote the elements of $S_{w_0w_0}$ as

$$S_{w_0w_{0(i,i)}} = S_{w_iw_i}, \quad S_{w_0w_{0(i,j)}} = S_{w_0w_{0(j,i)}} = S_{w_iw_j} = S_{w_jw_i}. \tag{2}$$

For later use, we define the $r \times r$ diagonal transfer function

$$Z(s) \triangleq \mathrm{diag}(z_1(s), z_2(s), \cdots, z_r(s)) \tag{3}$$

and the r-dimensional vectors

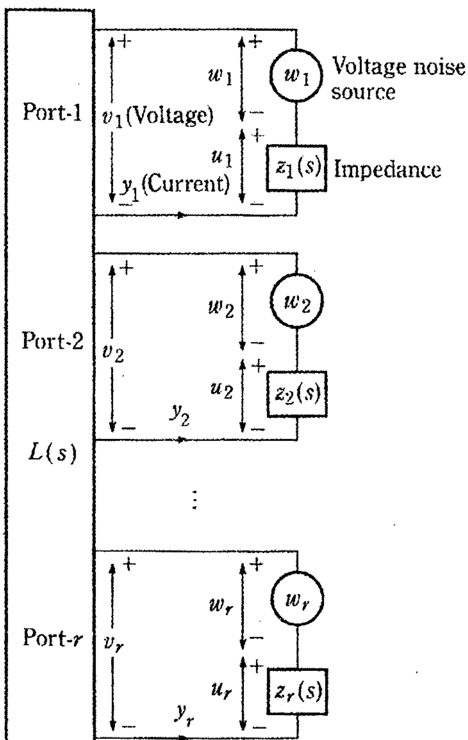

Fig. 1. Electrical representation of coupled impedance subsystems.

$$u_0 \triangleq [u_1 \cdots u_r]^T, \quad y_0 \triangleq [y_1 \cdots y_r]^T, \quad v_0 \triangleq [v_1 \cdots v_r]^T.$$

Thus, Fig. 1 can be recast as Fig. 2 in terms of $Z^{-1}(s)$, which is strictly positive real, and where $v_0 = Ly_0$ and $u_0 = w_0 - v_0$. Figure 2 will be useful in applying our results to mechanical systems for which v_0 denotes r force inputs and y_0 denotes r velocity outputs.

Next, we introduce three steady-state energy flows P_i^c, P_i^d, P_i^e, $i = 1, \cdots, r$, defined by

$P_i^c \triangleq$ the steady-state average energy flow entering the ith subsystem through the coupling $L(s)$,

$P_i^d \triangleq$ the steady-state average energy dissipation rate of the ith subsystem,

$P_i^e \triangleq$ the steady-state average external energy flow entering the ith subsystem.

As shown in Kishimoto and Bernstein (1995 a), P_i^c, P_i^d and P_i^e, $i = 1, \cdots, r$, are given by

$$P_i^c = -\frac{1}{2\pi}\int_{-\infty}^{\infty} \mathrm{Re}[L(j\omega)(L(j\omega)+Z(j\omega))^{-1} \times S_{w_0w_0}(L(j\omega)+Z(j\omega))^{-*}]_{(i,i)}d\omega, \tag{4}$$

$$P_i^d = -\frac{1}{2\pi}\int_{-\infty}^{\infty} \mathrm{Re}[Z(j\omega)(L(j\omega)+Z(j\omega))^{-1} \times S_{w_0w_0}(L(j\omega)+Z(j\omega))^{-*}]_{(i,i)}d\omega, \tag{5}$$

$$P_i^e = \frac{1}{2\pi}\int_{-\infty}^{\infty} \mathrm{Re}[S_{w_0w_0}(L(j\omega)+Z(j\omega))^{-*}]_{(i,i)}d\omega. \tag{6}$$

Energy balance at each subsystem implies that P_i^c, P_i^d and P_i^e satisfy

$$P_i^c + P_i^d + P_i^e = 0, \quad i = 1, \cdots, r. \tag{7}$$

Furthermore, if the coupling $L(s)$ is conservative (lossless), that is, $L(j\omega) + L^*(j\omega) = 0$, then,

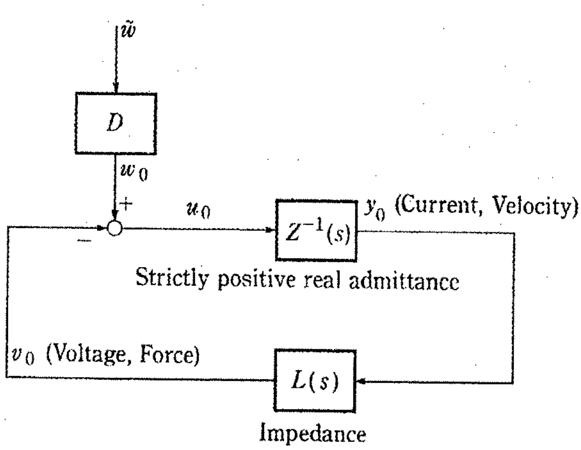

Fig. 2. Feedback representation of coupled electrical or mechanical subsystems.

$$\sum_{i=1}^{r} P_i^c = 0, \tag{8}$$

whereas if the coupling $L(s)$ is dissipative, that is, $L(j\omega) + L^*(j\omega) \geq 0$, then,

$$\sum_{i=1}^{r} P_i^c \leq 0. \tag{9}$$

As an example Fig. 3 illustrates the resulting energy flow model for the case $r = 3$.

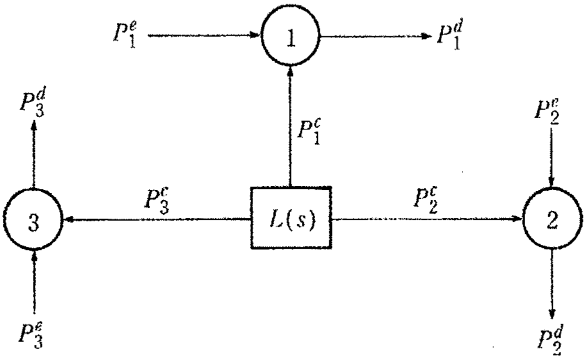

Fig. 3. Energy flow model with three subsystems.

3. LQG Positive Real Control Approach

In this section, we briefly review the LQG positive real control approach developed in Lozano-Leal and Joshi (1990). This result was recently extended to an H_2/H_∞ problem in Haddad et al. (1994), although this extension will not be needed here.

The LQG control approach provides the optimal controller for the following problem. Given the nth-order stabilizable and detectable plant

$$\dot{x}(t) = Ax(t) + Bu(t) + D_1\tilde{w}(t), \tag{10}$$

$$y(t) = Cx(t) + D_2\tilde{w}(t), \tag{11}$$

determine an nth-order dynamic feedback compensator $G_c(s) \sim \left[\begin{array}{c|c} A_c & B_c \\ \hline C_c & 0 \end{array}\right]$ of the form

$$\dot{x}_c(t) = A_c x_c(t) + B_c y(t), \tag{12}$$

$$u(t) = C_c x_c(t), \tag{13}$$

such that the closed-loop system (10)–(13) with dynamics matrix

$$\tilde{A} \triangleq \begin{bmatrix} A & BC_c \\ B_c C & A_c \end{bmatrix}$$

is asymptotically stable, and the H_2 performance index

$$J(A_c, B_c, C_c) = \lim_{t \to \infty} \mathscr{E}\left\{\frac{1}{t}\int_0^t [x^T(s)R_1x(s) + u^T(s)R_2u(s)]ds\right\} \tag{14}$$

$$= \|\tilde{G}(s)\|_2^2 \tag{15}$$

is minimized, where

$$\tilde{G}(s) \sim \left[\begin{array}{c|c} \tilde{A} & \tilde{D} \\ \hline \tilde{E} & 0 \end{array}\right]$$

is the closed-loop transfer function from the unit intensity white noise disturbance $\tilde{w}(t)$ to the performance variables

$$z(t) = E_1x(t) + E_2u(t), \tag{16}$$

and where $\tilde{D} \triangleq \begin{bmatrix} D_1 \\ B_c D_2 \end{bmatrix}$, $\tilde{E} \triangleq [E_1 \quad E_2C_c]$, $R_1 \triangleq E_1^T E_1$, $R_2 \triangleq E_2^T E_2 > 0$ and $E_1^T E_2 = 0$. It is assumed that A, B, C, D_1 and E_1 satisfy (i) (A, B) and (A, D_1) are stabilizable and (ii) (C, A) and (E_1, A) are detectable. Furthermore, for convenience, define $V_1 \triangleq D_1 D_1^T$, $V_2 \triangleq D_2 D_2^T > 0$, and assume that $D_1 D_2^T = 0$, which implies that the disturbance and the measurement noise are uncorrelated. The standard feedback representation of this control problem (Boyd and Barratt, 1991) is shown in Fig. 4.

For this problem, the optimal compensator (A_c, B_c, C_c) is given by

$$A_c = A - QC^TV_2^{-1}C - BR_2^{-1}B^TP, \tag{17}$$

$$B_c = QC^TV_2^{-1}, \tag{18}$$

$$C_c = -R_2^{-1}B^TP, \tag{19}$$

where Q and P are $n \times n$ nonnegative-definite matrices satisfying

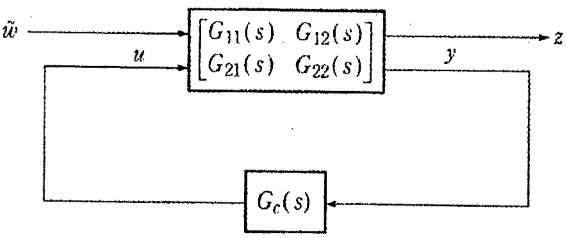

Fig. 4. Standard feedback representation.

$$AQ + QA^T + V_1 - QC^T V_2^{-1} CQ = 0, \tag{20}$$

$$A^T P + PA + R_1 - PBR_2^{-1} B^T P = 0. \tag{21}$$

Next, we assume that the plant (10), (11) is positive real. For positive real plants, a strictly positive real controller is desirable since the negative-feedback closed-loop system is guaranteed to be asymptotically stable (Benhabib et al., 1981). The controller obtained above, however, is not necessarily strictly positive real. For this problem, Theorem 1 of Lozano-Leal and Joshi (1990) can be used to obtain an nth-order strictly positive real compensator $-G_c(s) \sim \left[\begin{array}{c|c} A_c & B_c \\ \hline -C_c & 0 \end{array}\right]$ that minimizes the H_2 performance index $J(A_c, B_c, C_c)$. Since the plant $G(s) \sim \left[\begin{array}{c|c} A & B \\ \hline C & 0 \end{array}\right]$ is positive real, there exists a positive-definite matrix Q_0 satisfying (Anderson and Vongpanitlerd, 1973)

$$AQ_0 + Q_0 A^T = -LL^T, \tag{22}$$

$$Q_0 C^T = B. \tag{23}$$

As shown in Lozano-Leal and Joshi (1990), if the LQG weights V_1, V_2, R_1, R_2 are chosen according to

$$V_1 = LL^T + BR_2^{-1} B^T > 0, \tag{24}$$

$$V_2 = R_2 > 0, \tag{25}$$

$$R_1 > C^T V_2^{-1} C, \tag{26}$$

then the dynamic compensator $-G_c(s)$ given by (17), (18) and (19) is strictly positive real. With $-G_c(s)$, the negative feedback closed-loop system matrix $\tilde{A}$ is now asymptotically stable as explained above.

In the following sections, we consider two types of energy flow control problems in which the plant is positive real. In each case, we design positive real controllers by means of the above approach.

4. Design of an Energy Flow Controller as an Additional Interconnected Subsystem

In this section, we consider a control problem involving $r-1$ subsystems $z_i(s)$ interconnected by a conservative coupling. In this problem, we assume that the controller $G_c(s) = z_c^{-1}(s)$ can interact with the subsystems only through additional coupling elements. Thus, the controller can be treated as an additional rth subsystem. This situation can be viewed as representative of a large space structure with appendages that are interconnected by a central support structure. The controller can then be realized as an active or passive device that is also connected to the central support structure. The transfer functions $Z_z^{-1}(s) = \mathrm{diag}(z_1^{-1}(s), \cdots, z_{r-1}^{-1}(s))$ and $z_c^{-1}(s)$ are assumed to be expressed by the state space models

$$\dot{x}_z(t) = A_z x_z(t) + B_z u_z(t), \tag{27}$$

$$y_z(t) = C_z x_z(t), \tag{28}$$

$$\dot{x}_c(t) = A_c x_c(t) + B_c y(t), \tag{29}$$

$$u(t) = C_c x_c(t), \tag{30}$$

respectively, where $x_z(t) \in \mathscr{R}^{n_z}$, $x_c(t) \in \mathscr{R}^{n_c}$, $y_z(t) \in \mathscr{R}^{r-1}$, $u_z(t) \in \mathscr{R}^{r-1}$ and $y(t)$, $u(t)$ are scalars. As shown in Fig. 5, $Z^{-1}(s)$ in Fig. 2 is now comprised of both $Z_z^{-1}(s)$ and $z_c^{-1}(s)$, that is, $Z(s) = \mathrm{diag}(z_1(s), \cdots, z_{r-1}(s), z_c(s))$, so that the total number of subsystems is r. Furthermore, $y_0(t)$ and $u_0(t)$ in Fig. 5 are given by

$$y_0 = \begin{bmatrix} y_z \\ u \end{bmatrix}, \quad u_0 = \begin{bmatrix} u_z \\ y \end{bmatrix}.$$

After the controller is connected, the lossless coupling $L(s)$ is expressed by the state space model

$$\dot{x}_L(t) = A_L x_L(t) + B_L y_0(t), \tag{31}$$

$$v_0(t) = C_L x_L(t), \tag{32}$$

where $x_L(t) \in \mathscr{R}^{n_L}$ and $v_0(t) \in \mathscr{R}^r$.

We assume that no disturbance enters $z_c^{-1}(s)$. Therefore, w_0 in Fig. 2 is given by

$$w_0 = \begin{bmatrix} w \\ 0 \end{bmatrix} = D\tilde{w}, \tag{33}$$

where $w(t) \triangleq [w_1(t) \cdots w_{r-1}(t)]^T$ and

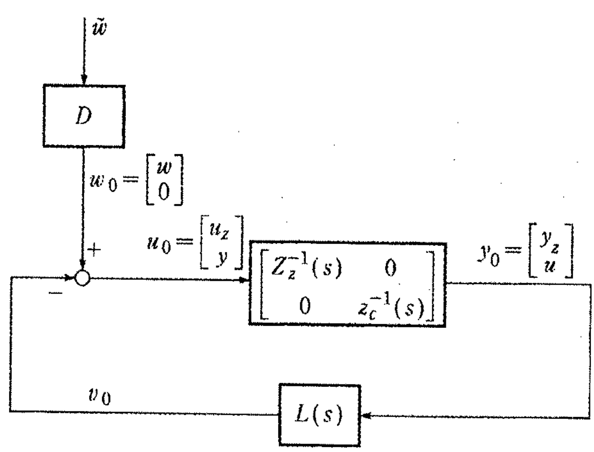

Fig. 5. Feedback representation of plant and controller.

$$D \triangleq \begin{bmatrix} D_{11} \\ 0_{1\times d} \end{bmatrix} \in \mathscr{R}^{r\times d},$$

and where $D_{11} \in \mathscr{R}^{(r-1)\times d}$. Since $u_0(t) = w_0(t) - v_0(t)$ it follows that

$$u_0 = \begin{bmatrix} u_z \\ y \end{bmatrix} = \begin{bmatrix} w \\ 0 \end{bmatrix} - v_0,$$

which implies that $u_z(t)$ is the force vector resulting from the difference of the disturbance forces and the coupling forces, while $y(t)$ represents the coupling force only as shown in Fig. 5.

With this notation and the above equations the feedback system shown in Fig. 5 is obtained by

$$\dot{\tilde{x}}(t) = \tilde{A}\tilde{x}(t) + \tilde{D}\tilde{w}(t), \tag{34}$$

where

$$\tilde{x}(t) \triangleq \begin{bmatrix} x_z(t) \\ x_L(t) \\ x_c(t) \end{bmatrix}, \quad \tilde{A} \triangleq \begin{bmatrix} A_z & -B_z C_{L1} & 0 \\ B_{L1} C_z & A_L & B_{L2} C_c \\ 0 & -B_c C_{L2} & A_c \end{bmatrix}, \quad \tilde{D} \triangleq \begin{bmatrix} B_z D_{11} \\ 0 \\ 0 \end{bmatrix},$$

and $B_{L1} \in \mathscr{R}^{n_L \times (r-1)}$, $B_{L2} \in \mathscr{R}^{n_L}$, $C_{L1} \in \mathscr{R}^{(r-1)\times n_L}$ and $C_{L2} \in \mathscr{R}^{1\times n_L}$ are obtained by partitioning B_L and C_L as

$$B_L = [B_{L1} \quad B_{L2}], \quad C_L = \begin{bmatrix} C_{L1} \\ C_{L2} \end{bmatrix}.$$

We now determine A_c, B_c and C_c in (29) and (30) by means of the LQG positive real approach described in Sec. 3. By defining

$$x(t) \triangleq \begin{bmatrix} x_z(t) \\ x_L(t) \end{bmatrix}, \quad A \triangleq \begin{bmatrix} A_z & -B_z C_{L1} \\ B_{L1} C_z & A_L \end{bmatrix} \in \mathscr{R}^{(n_z+n_L)\times(n_z+n_L)},$$

$$B \triangleq \begin{bmatrix} 0 \\ B_{L2} \end{bmatrix} \in \mathscr{R}^{(n_z+n_L)}, \quad C \triangleq [0 \quad -C_{L2}] \in \mathscr{R}^{1\times(n_z+n_L)},$$

$$D_1 \triangleq \begin{bmatrix} B_z D_{11} \\ 0 \end{bmatrix} \in \mathscr{R}^{(n_z+n_L)\times r},$$

then $\tilde{A}$ and $\tilde{D}$ in (34) have the same form as in the LQG problem, where D_2 in $\tilde{D}$ represents fictitious measurement noise required by the LQG approach. Thus, (A, B, C) can be viewed as a realization of the plant $G_{22}(s)$ in Fig. 4.

The controller is now required to maximize the energy flow from the ith subsystem, that is, to maximize $-P_i^c$. By defining

$$C_1 \triangleq \begin{bmatrix} C_z & 0_{(r-1)\times n_L} & 0_{(r-1)\times(n_z+n_L)} \\ 0_{1\times n_z} & 0_{1\times n_L} & C_c \end{bmatrix} \in \mathscr{R}^{r\times 2(n_z\times n_L)},$$

P_i^e in (6) is given by Kishimoto and Bernstein (1995 a)

$$P_i^e = \frac{1}{2}[D\tilde{D}^T C_1^T]_{(i,i)}. \tag{35}$$

Thus, P_i^e is constant and independent of the controller gains. In fact, for the special case in which each subsystem is a second-order system, P_i^e in (35) is given by $P_i^e = S_{w_i w_i}/2m_i$, where m_i is the mass of the ith subsystem (Woodhouse, 1981). It thus follows from (7) that maximizing $-P_i^c$ is equivalent to minimizing $-P_i^d$.

To express the dissipation of the ith subsystem P_i^d in terms of the steady state covariance $\tilde{Q} \triangleq \lim_{t\to\infty} \mathscr{E}[x(t)x^T(t)]$, we now assume that each subsystem $z_i(s)$ has constant real part c_i and define

$$C_d \triangleq \mathrm{diag}(c_1, \cdots, c_{r-1}, 0) \in \mathscr{R}^{r\times r}. \tag{36}$$

Then P_i^d, $i = 1, \cdots, r-1$, defined by (5) can be obtained by (Kishimoto and Bernstein, 1995 a)

$$\begin{aligned}
P_i^d &= \frac{-1}{2\pi}\left(\int_{-\infty}^{\infty} \mathrm{Re}[Z(j\omega)(L(j\omega)+Z(j\omega))^{-1} S_{w_0 w_0}(L(j\omega)+Z(j\omega))^{-*}]d\omega\right)_{(i,i)} \\
&= \frac{-1}{2\pi}\left[\int_{-\infty}^{\infty} C_d(L(j\omega)+Z(j\omega))^{-1} DD^T(L(j\omega)+Z(j\omega))^{-*}d\omega\right]_{(i,i)} \\
&= \frac{-1}{2\pi}\left[C_d\int_{-\infty}^{\infty} (L(j\omega)+Z(j\omega))^{-1} DD^T(L(j\omega)+Z(j\omega))^{-*}d\omega\right]_{(i,i)} \\
&= -\left(C_d \frac{1}{2\pi}\int_{-\infty}^{\infty} [C_1(j\omega I - \tilde{A})^{-1}\tilde{D}][C_1(j\omega I - \tilde{A})^{-1}\tilde{D}]^* d\omega\right)_{(i,i)} \\
&= -(C_d C_1 \tilde{Q} C_1^T)_{(i,i)},
\end{aligned}$$

where $\tilde{Q}$ satisfies the Lyapunov equation

$$0 = \tilde{A}\tilde{Q} + \tilde{Q}\tilde{A}^T + \tilde{D}\tilde{D}^T. \tag{37}$$

Thus, the cost $-P_i^d$ to be minimized is given by

$$-P_i^d = (C_d C_1 \tilde{Q} C_1^T)_{(i,i)}. \tag{38}$$

Now using the definition of $\tilde{Q}$ yields

$$\begin{aligned}
-P_i^d &= [C_d C_1(\lim_{t\to\infty} \mathscr{E}[x(t)x^T(t)])C_1^T]_{(i,i)} \\
&= \lim_{t\to\infty} \mathscr{E}[e_i^T C_d C_1 x(t)x^T(t)C_1^T e_i] \\
&= \lim_{t\to\infty} \mathscr{E}[\mathrm{tr}[e_i^T C_d C_1 x(t)x^T(t)C_1^T e_i]] \\
&= \lim_{t\to\infty} \mathscr{E}[\mathrm{tr}[x^T(t)C_1^T e_i e_i^T C_d C_1 x(t)]] \\
&= \lim_{t\to\infty} \mathscr{E}[x^T(t)C_1^T e_i c_i e_i^T C_1 x(t)].
\end{aligned} \tag{39}$$

Thus, letting the performance matrix E_1 in (16) be given by

$$E_1 = \sqrt{c_i}\, e_i^T C_1 \tag{40}$$

corresponds to minimizing $-P_i^d$.

In order to guarantee closed-loop stability, we need to show that the controlled plant $G_{22}(s)$ is positive real. By partitioning the stiffness coupling $L(s)$ in (46) as

$$L(s)=\begin{bmatrix} L_{11}(s) & L_{12}(s) \\ L_{21}(s) & L_{22}(s) \end{bmatrix}, \tag{41}$$

it can be shown that $G_{11}(s)$, $G_{12}(s)$, $G_{21}(s)$ and $G_{22}(s)$ in Fig. 4 are given by

$$G_{11}(s) \triangleq \sqrt{c_i}\, e_i^T (Z_z(s)+L_{11}(s))^{-1}, \tag{42}$$

$$G_{12}(s) \triangleq \sqrt{c_i}\, e_i^T (Z_z(s)+L_{11}(s))^{-1} L_{12}(s) - E_2, \tag{43}$$

$$G_{21}(s) \triangleq -L_{21}(s)(Z_z(s)+L_{11}(s))^{-1}, \tag{44}$$

$$\begin{aligned} G_{22}(s) &\triangleq L_{22}(s) - L_{21}(s)(I+Z_z^{-1}(s)L_{11}(s))^{-1} Z_z^{-1}(s) L_{12}(s) \\ &= L_{22}(s) - L_{21}(s)(Z_z(s)+L_{11}(s))^{-1} L_{12}(s). \end{aligned} \tag{45}$$

Since $L(j\omega)+L^*(j\omega)=0$, it follows that

$$L_{11}(j\omega)+L_{11}^*(j\omega)=0, \quad L_{22}(j\omega)+L_{22}^*(j\omega)=0, \quad L_{12}(j\omega)=-L_{21}^*(j\omega).$$

Furthermore, from the fact that $Z_z(s)$ is strictly positive real, we have $Z_z(s) + Z_z^*(s) > 0$ for $\mathrm{Re}[s]>0$. These relations imply

$$\begin{aligned} &G_{22}(j\omega)+G_{22}^*(j\omega) \\ &\quad = L_{22}(j\omega) - L_{21}(j\omega)(Z_z(j\omega)+L_{11}(j\omega))^{-1} L_{12}(j\omega) \\ &\qquad + [L_{22}(j\omega) - L_{21}(j\omega)(Z_z(j\omega)+L_{11}(j\omega))^{-1} L_{12}(j\omega)]^* \\ &\quad = -L_{21}(j\omega)(Z_z(j\omega)+L_{11}(j\omega))^{-1} L_{12}(j\omega) \\ &\qquad - L_{12}^*(j\omega)(Z_z(j\omega)+L_{11}(j\omega))^{-*} L_{21}^*(j\omega) \\ &\quad = -L_{21}(j\omega)(Z_z(j\omega)+L_{11}(j\omega))^{-*} \\ &\qquad \times [(Z_z(j\omega)+L_{11}(j\omega))^* + (Z_z(j\omega)+L_{11}(j\omega))] \\ &\qquad \times (Z_z(j\omega)+L_{11}(j\omega))^{-1} L_{12}(j\omega) \\ &\quad = -L_{21}(j\omega)(Z_z(j\omega)+L_{11}(j\omega))^{-*}(Z_z(j\omega)+Z_z^*(j\omega)) \\ &\qquad \times (Z_z(j\omega)+L_{11}(j\omega))^{-1} L_{12}(j\omega) \\ &\quad = L_{12}^*(j\omega)(Z_z(j\omega)+L_{11}(j\omega))^{-*}(Z_z(j\omega)+Z_z^*(j\omega)) \\ &\qquad \times (Z_z(j\omega)+L_{11}(j\omega))^{-1} L_{12}(j\omega) \\ &\quad \geq 0. \end{aligned}$$

Thus the plant $G_{22}(s)$ is positive real. This fact can also be explained as follows. If the plant $G_{22}(s)$ is not positive real, then the Nyquist plot contour intersects the left half plane. When a suitable strictly positive real controller $z_c^{-1}(s)$ is applied to such a system, the loop gain is increased and the contour encircles

$-1+j0$, which destabilizes the closed-loop system. This contradicts the fact that the feedback system shown in Fig. 5 is asymptotically stable for every strictly positive real controller $z_c(s)$ (Kishimoto and Bernstein, 1995 a). Since the plant $G_{22}(s)$ is positive real, the results in Sec. 3 can be used to determine an optimal strictly positive real compensator $z_c^{-1}(s)$.

We now specialize the above results to the case of stiffness coupling. By setting $A_L=0$ and $B_L=I$ in (31), the stiffness coupling $L(s)$ is given by

$$L(s)=\frac{1}{s}C_L, \tag{46}$$

where the $r\times r$ symmetric matrix C_L is partitioned as

$$C_L \triangleq \begin{bmatrix} C_{L11} & C_{L12} \\ C_{L12}^T & C_{L22} \end{bmatrix} \tag{47}$$

and $C_{L11}\in\mathcal{R}^{(r-1)\times(r-1)}$. Note that the dimension of the state space vector $x_L(t)$ for the coupling $L(s)$ is now $n_L=r$.

Furthermore, we assume that x_z in (27) consists of both positions and velocities so that there exists an output matrix C_p such that

$$\int y_z dt = C_p x_z. \tag{48}$$

Then from (31), (32) and (48), it follows that

$$\int y_0 dt = \begin{bmatrix} \int y_z dt \\ \int u dt \end{bmatrix} = \begin{bmatrix} C_p x_z \\ x_{pc} \end{bmatrix}, \tag{49}$$

where a scalar state $x_{pc}(t)$ is defined by

$$\dot{x}_{pc}(t)\triangleq u(t). \tag{50}$$

Hence, with $x_L\triangleq[(C_p x_z)^T \quad x_{pc}^T]^T$

$$v_0 = C_L x_L = C_L\begin{bmatrix} C_p x_z \\ x_{pc} \end{bmatrix}. \tag{51}$$

By substituting the $r\times r$ matrices $A_L=0$, $B_L=I$ and (51) into (34), we obtain the feedback system shown in Fig. 5 with

$$\dot{\tilde{x}}(t)=\tilde{A}\tilde{x}(t)+\tilde{D}\tilde{w}(t), \tag{52}$$

where

$$\tilde{x}(t)\triangleq\begin{bmatrix} x_z(t) \\ x_{pc}(t) \\ x_c(t) \end{bmatrix}, \quad \tilde{A}\triangleq\begin{bmatrix} A_z - B_z C_{L11} C_p & -B_z C_{L12} & 0 \\ 0 & 0 & C_c \\ -B_c C_{L12}^T C_p & -B_c C_{L22} & A_c \end{bmatrix}, \quad \tilde{D}\triangleq\begin{bmatrix} B_z D_{11} & 0 \\ 0 & 0 \\ 0 & 0 \end{bmatrix}.$$

Note that as shown in (51) the first $r-1$ elements of $x_L(t)$ are given by $C_p x_z(t)$, which depends on $x_z(t)$. Therefore, since only the rth element $x_{pc}(t)$ of $x_L(t)$ in (34) is included in the state of the augmented feedback expression (52), it follows that the dimension of $\tilde{x}(t)$ is $2(n_z+1)$ rather than $2(n_z+n_L)$.

By defining

$$A \triangleq \begin{bmatrix} A_z - B_z C_{L11} C_p & -B_z C_{L12} \\ 0 & 0 \end{bmatrix} \in \mathscr{R}^{(n_z+1)\times(n_z+1)},$$

$$B \triangleq [0 \cdots 0 \quad 1]^T \in \mathscr{R}^{n_z+1}, \quad C \triangleq [-C_{L12}^T C_p \quad -C_{L22}] \in \mathscr{R}^{1\times(n_z+1)},$$

$$D_1 \triangleq \begin{bmatrix} B_z D_{11} & 0 \\ 0 & 0 \end{bmatrix} \in \mathscr{R}^{(n_z+1)\times r},$$

it follows that $\tilde{A}$ and $\tilde{D}$ in (52) have the same form as the LQG problem. Thus, we can design a positive real controller (A_c, B_c, C_c) that minimizes $-P_i^d$ in the same manner as above.

As an illustrative numerical example we consider the three coupled oscillator system with controller as shown in Fig. 6, where $k_1=3.5$, $k_2=2.5$, $k_3=1$, $m_1=1$, $m_2=2$, $m_3=3$, $K_{12}=0.5$, $K_{13}=0.6$, $K_{23}=0.7$, $K_{1c}=0.8$, $K_{2c}=0.9$, $K_{3c}=1.0$ and $c_1=0.1$, $c_2=0.2$, $c_3=0.3$. Furthermore, let the white noise disturbances $w_i(t)$, $i=1,2,3$, have unit intensity $S_{w_i w_i}=1$ so that $D=\mathrm{diag}(1,1,1,0)$. To maximize $-P_i^c$, $i=1,2,3$, we set $E_2=0.1$ in (16). The resulting energy flow diagrams calculated by means of the steady state covariance (Kishimoto and Bernstein, 1995 a) are illustrated in Fig. 7, where OL denotes the open-loop system and G_{c1}, G_{c2} and G_{c3} represent the controllers designed to maximize $-P_1^c$, $-P_2^c$ and $-P_3^c$, respectively. Figure 7 shows that the controller absorbs energy from all of the subsystems and reduces the energy dissipation from each subsystem. Note that in Fig. 7 the signs of the energy flows correspond to the arrows in the figure. For example, energy flow into oscillator 3 in

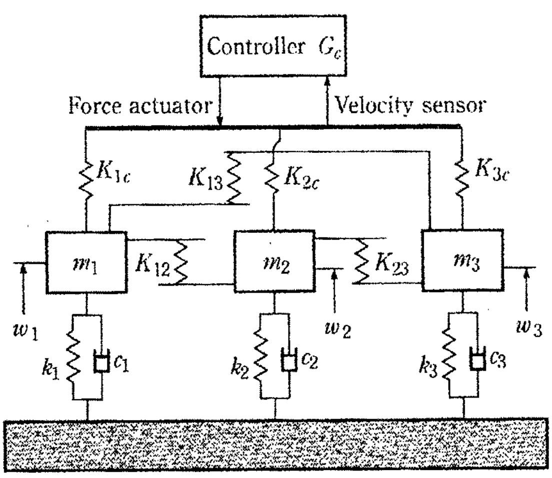

Fig. 6. Three coupled oscillator system with controller.

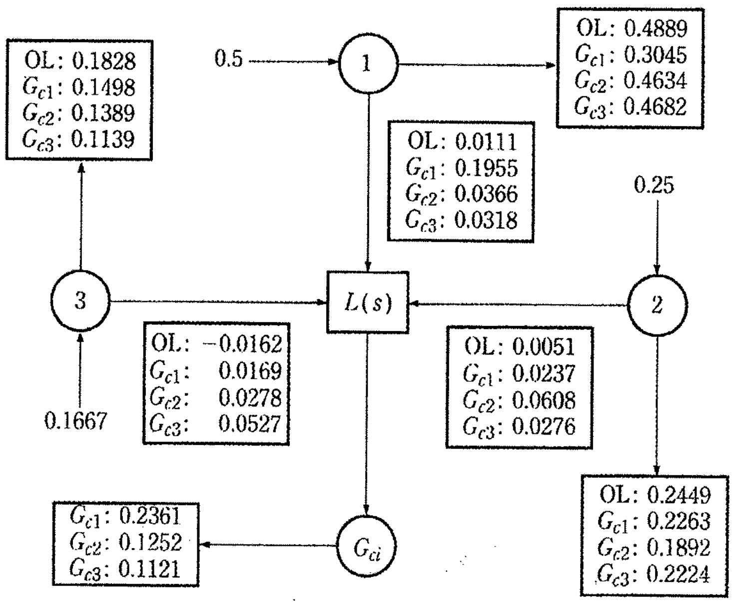

Fig. 7. Energy flow among oscillators for the open-loop system and for the closed-loop system with controllers G_{c1}, G_{c2} and G_{c3}.

the open-loop system is reversed after controller G_{ci} is applied. Furthermore, it can be seen that the controller G_{ci} maximizes energy flow from the ith subsystem and thus minimizes the energy dissipated by the ith subsystem.

To examine the actual reduction of vibration by these controllers, we define the steady-state stored energy by

$$\mathscr{E}_i \triangleq \frac{1}{2} m_i \mathscr{E}[\dot{x}_i^2(t)] + \frac{1}{2} k_i \mathscr{E}[x_i^2(t)], \quad i = 1, 2, 3, \tag{53}$$

where $x_i(t)$ and $\dot{x}_i(t)$ are the displacement and the velocity of the ith oscillator, respectively. Table 1 shows that each controller G_{ci} successfully reduces the stored energy $\mathscr{E}_i$ of the corresponding ith oscillator. For example, controller G_{c1} reduces the stored energy of oscillator 1 to 48.32 percent of its open-loop value.

Table 1. Steady-state stored energy for three coupled oscillators

Stored energy	Open-loop	Controller 1	Controller 2	Controller 3
$\mathscr{E}_1$	4.2936	2.0747 (48.32[%])	3.5476 (82.63[%])	3.8208 (88.99[%])
$\mathscr{E}_2$	2.0556	1.5775 (76.74[%])	0.9772 (47.54[%])	1.6290 (79.25[%])
$\mathscr{E}_3$	1.3458	0.8542 (63.47[%])	0.7809 (58.02[%])	0.6374 (42.24[%])

Gain and phase plots of the controllers are shown in Fig. 8, which shows that the gain plot of controller G_{c1} has a peak near the coupled natural frequency of oscillator 1, that is, $\omega_1 = (k_1 + k_{12} + k_{13} + k_{1c})/m_1 = 2.3238$ [rad/sec]. Similarly, controller G_{c2} has a gain peak near $\omega_2 = 1.516$ [rad/sec], while controller G_{c3} has a gain peak near $\omega_3 = 1.048$ [rad/sec]. These controllers are strictly positive real since their phase plots lie in the range $(-90°, 90°)$.

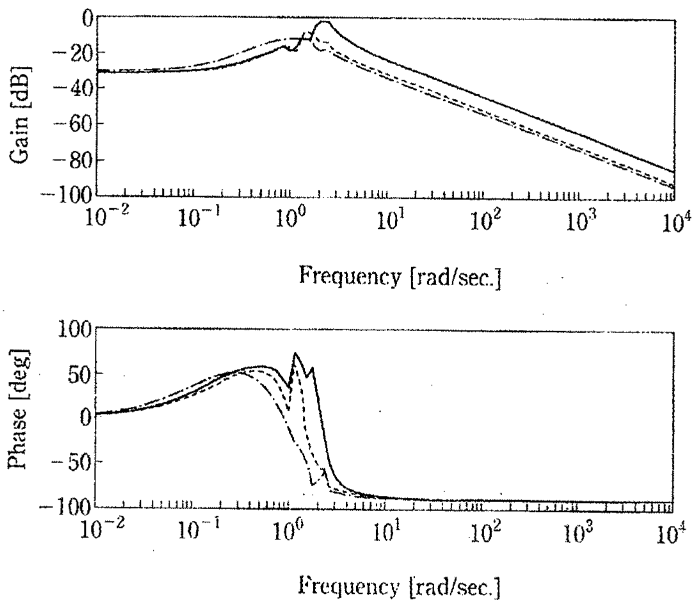

Fig. 8. Magnitude and phase of controllers G_{c1} (solid), G_{c2} (dashed), G_{c3} (dash-dot).

5. Design of an Energy Flow Controller as a Dissipative Coupling

In the previous section, we considered the subsystem interconnection explicitly in the energy flow analysis. As an alternative approach, we view the structure as a collection of uncoupled subsystems, such as modes, which become coupled only by means of the feedback controller. In contrast to the previous section, in which the control is applied to the flexible structure only through the conservative coupling, we now assume that the control force can be applied to the structure directly and design a controller to regulate energy flow among structural modes.

Consider a structure subject to unit intensity white noise disturbances $\tilde{w}_i(t)$, $i = 1, \cdots, d$, applied at locations $\hat{\xi}_i$. The ith actuator located at ξ_i, $i = 1, \cdots, m$, applies a control force $u_i(t)$. Our goal is to design a controller that maximizes energy flow from the ith structural mode. For this purpose we consider each mode as a subsystem to obtain the feedback system corresponding to Fig. 1 and design a dissipative controller as a dissipative coupling.

First, we denote the modal decomposition of the structure by

$$\chi(\xi, t) = \sum_{i=1}^{\infty} q_i(t)\psi_i(\xi), \tag{54}$$

where $q_i(t)$ denotes modal coordinates and $\psi_i(\xi)$ denotes orthogonal eigenfunctions. Then, using the boundary conditions and orthogonality properties, it follows that the modal coordinates $q_j(t)$ satisfy

$$\ddot{q}_j(t) + 2\zeta_j\omega_j\dot{q}_j(t) + \omega_j^2 q_j(t) = \sum_{l=1}^{m} \psi_j(\xi_l)u_l(t) + \sum_{l=1}^{d} \psi_j(\hat{\xi}_l)\tilde{w}_l(t), \tag{55}$$

where we assume proportional damping $2\zeta_j\omega_j$. From (54), $\dot{\chi}(\xi_i, t)$ is the velocity of the structure at the ith actuator position ξ_i and we assume that m velocity sensors are also located at these positions. Hence, the m sensors and m actuators are colocated and dual.

Now we consider r structural modes and define

$$x(t) \triangleq [q_1(t) \quad \dot{q}_1(t) \quad q_2(t) \quad \dot{q}_2(t) \cdots q_r(t) \quad \dot{q}_r(t)]^T,$$

$$u(t) \triangleq [u_1(t) \quad u_2(t) \cdots u_m(t)]^T,$$

$$\tilde{w}(t) \triangleq [\tilde{w}_1(t) \quad \tilde{w}_2(t) \cdots \tilde{w}_r(t)]^T,$$

$$y(t) \triangleq [\dot{\chi}(\xi_1, t) \quad \dot{\chi}(\xi_2, t) \cdots \dot{\chi}(\xi_r, t)]^T.$$

Then from (54), we obtain the state space model

$$\dot{x}(t) = Ax(t) + Bu(t) + D\tilde{w}(t), \tag{56}$$

$$y(t) = B^T x(t), \tag{57}$$

where

$$A \triangleq \operatorname*{block-diag}_{i=1,\cdots,r}\begin{bmatrix} 0 & 1 \\ -\omega_i^2 & -2\zeta_i\omega_i \end{bmatrix} \in \mathscr{R}^{2r\times 2r},$$

$$B \triangleq \begin{bmatrix} 0 & \cdots & 0 \\ \psi_1(\xi_1) & \cdots & \psi_1(\xi_m) \\ 0 & \cdots & 0 \\ \psi_2(\xi_1) & \cdots & \psi_2(\xi_m) \\ \vdots & \vdots & \vdots \\ 0 & \cdots & 0 \\ \psi_r(\xi_1) & \cdots & \psi_r(\xi_m) \end{bmatrix} \in \mathscr{R}^{2r\times m}, \quad D \triangleq \begin{bmatrix} 0 & \cdots & 0 \\ \psi_1(\hat{\xi}_1) & \cdots & \psi_1(\hat{\xi}_d) \\ 0 & \cdots & 0 \\ \psi_2(\hat{\xi}_1) & \cdots & \psi_2(\hat{\xi}_d) \\ \vdots & \vdots & \vdots \\ 0 & \cdots & 0 \\ \psi_r(\hat{\xi}_1) & \cdots & \psi_r(\hat{\xi}_d) \end{bmatrix} \in \mathscr{R}^{2r\times d}.$$

To obtain the feedback system equivalent to Fig. 2 we introduce the diagonal matrix B_0 defined by

$$B_0 \triangleq \operatorname{diag}(0, 1, 0, 1, \cdots, 0, 1) \in \mathscr{R}^{2r\times 2r},$$

and define

$$Z^{-1}(s) \sim \left[\begin{array}{c|c} A & B_0 \\ \hline B_0 & 0 \end{array}\right], \tag{58}$$

$$y_0(t) \triangleq B_0 x(t) \in \mathscr{R}^{2r}, \tag{59}$$

$$w_0(t) \triangleq D\tilde{w}(t) \in \mathscr{R}^{2r}, \tag{60}$$

$$v_0(t) \triangleq -Bu(t) \in \mathscr{R}^{2r}. \tag{61}$$

We thus obtain Fig. 9 where the coupling $L(s)$ is defined by

$$L(s) \triangleq -BG_c(s)B^T. \tag{62}$$

Now using the LQG positive real approach we design a strictly positive real controller $G_c(s)$ satisfying

$$G_c(s) + G_c^*(s) < 0, \quad \mathrm{Re}[s] > 0, \tag{63}$$

so that $L(s)$ satisfies

$$\begin{aligned} L(s) + L^*(s) &= -BG_c(s)B^T - [BG_c(s)B^T]^* \\ &= -B[G_c(s) + G_c^*(s)]B^T \\ &\geq 0 \end{aligned} \tag{64}$$

for $\mathrm{Re}[s] > 0$. Thus the coupling $L(s)$ serves as a dissipative controller which controls the energy flow among the structural modes. Our goal is to design $G_c(s)$ so that $L(s)$ maximizes energy flow from a specified mode.

Next we consider a realization of the feedback system in Fig. 9. The transfer functions $Z^{-1}(s)$ and $G_c(s)$ are expressed by the state space models

$$\dot{x}(t) = Ax(t) + B_0 u_0(t), \tag{65}$$

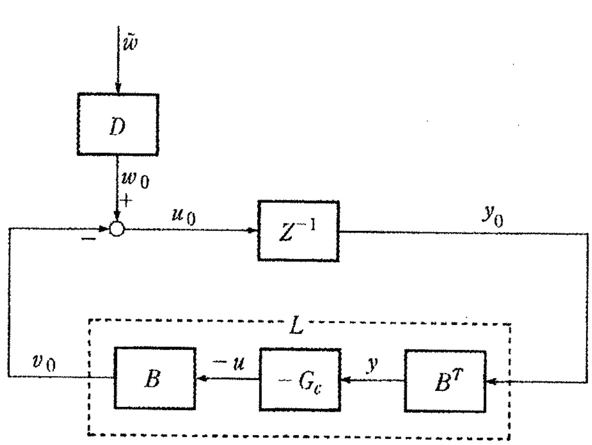

Fig. 9. Feedback representation of coupled structural modes.

$$y_0(t) = B_0 x(t), \tag{66}$$

$$\dot{x}_c(t) = A_c x_c(t) + B_c y(t), \tag{67}$$

$$u(t) = C_c x_c(t), \tag{68}$$

respectively. Since $u_0 = w_0 - v_0$ and $B_0 B = B$, it follows from (56), (57) (65)–(68) that

$$\dot{x}(t) = Ax(t) + BC_c x_c(t) + B_0 w_0(t), \tag{69}$$

$$\dot{x}_c(t) = A_c x_c(t) + B_c B^T x(t). \tag{70}$$

Thus, the feedback system (69) and (70) is given by

$$\dot{\tilde{x}}(t) = \tilde{A}\tilde{x}(t) + \tilde{D}\tilde{w}(t), \tag{71}$$

where

$$\tilde{x}(t) \triangleq \begin{bmatrix} x(t) \\ x_c(t) \end{bmatrix} \in \mathscr{R}^{4r}, \quad \tilde{A} \triangleq \begin{bmatrix} A & BC_c \\ B_c B^T & A_c \end{bmatrix} \in \mathscr{R}^{4r\times 4r},$$
$$\tilde{D} \triangleq \begin{bmatrix} B_0 D \\ B_c D_2 \end{bmatrix} \in \mathscr{R}^{4r\times 2r}.$$

By setting $C = B^T$ in (11), it can be seen that $\tilde{A}$ has the usual closed-loop structure.

Now we choose the performance variable in (16) to maximize energy flow from the ith structural mode, that is, to maximize $-P_i^c$. By the same argument as in the previous section, this is equivalent to minimizing $-P_i^d$.

From Fig. 9, we obtain

$$y_0 = (L(s) + Z(s))^{-1} w_0 = C_{1a}(sI - \tilde{A})^{-1} B_0 D\tilde{w}, \tag{72}$$

where

$$C_{1a} \triangleq [B_0 \quad 0_{2r\times 2r}] \in \mathscr{R}^{2r\times 4r}. \tag{73}$$

Furthermore, by defining the $2r \times 2r$ damping matrix C_{da} as

$$C_{da} \triangleq \mathrm{diag}(0, 2\zeta_1\omega_1, 0, 2\zeta_2\omega_2, \cdots, 0, 2\zeta_r\omega_r), \tag{74}$$

then P_i^d, $i = 1, \cdots, r$, defined by (5) is given by

$$P_i^d = -(C_{da} C_{1a} \tilde{Q} C_{1a}^T)_{(2i,2i)}, \tag{75}$$

where $\tilde{Q}$ satisfies the Lyapunov equation

$$0 = \tilde{A}\tilde{Q} + \tilde{Q}\tilde{A}^T + \tilde{D}\tilde{D}^T. \tag{76}$$

Thus, the performance index to be minimized is given by $(C_{da} C_{1a} \tilde{Q} C_{1a}^T)_{(2i,2i)}$ as in the previous section. Furthermore, since

$$\begin{aligned}(C_{da}C_{1a}\tilde{Q}C_{1a}^T)_{(2i,2i)} &= [C_{da}C_{1a}(\lim_{t\to\infty}\mathscr{E}[x(t)x^T(t)])C_{1a}^T]_{(2i,2i)} \\ &= \lim_{t\to\infty}\mathscr{E}[e_{2i}^T C_{da}C_{1a}x(t)x^T(t)C_{1a}^T e_{2i}] \\ &= \lim_{t\to\infty}\mathscr{E}[\mathrm{tr}[e_{2i}^T C_{da}C_{1a}x(t)x^T(t)C_{1a}^T e_{2i}]] \\ &= \lim_{t\to\infty}\mathscr{E}[\mathrm{tr}[x^T(t)C_{1a}^T e_{2i}e_{2i}^T C_{da}C_{1a}x(t)]] \\ &= \lim_{t\to\infty}\mathscr{E}[x^T(t)C_{1a}^T e_{2i}C_{da(2i,2i)}e_{2i}^T C_{1a}x(t)], \end{aligned} \tag{77}$$

the performance matrix E_1 needed in (16) to maximize energy flow from the ith mode is given by

$$E_1 = \sqrt{C_{da(2i,2i)}}\, e_i^T C_{1a} = \sqrt{2\zeta_i\omega_i}\, e_i^T C_{1a}. \tag{78}$$

Finally, since (56) and (57) comprise a state space model of the structure given by (55), it follows that the plant (A, B, C) is strictly positive real. We can thus obtain a strictly positive real controller $-G_c(s)$ in the same manner as in the previous section.

As a numerical example, we now consider the simply supported uniform Bernoulli-Euler beam of length L in Fig. 10. The partial differential equation for the transverse deflection $\chi(\xi, t)$ is given by

$$\rho\frac{\partial^2\chi(\xi,t)}{\partial t^2} + \frac{\partial^2}{\partial\xi^2}\left[EI_A\frac{\partial^2\chi(\xi,t)}{\partial\xi^2}\right] = \sum_{i=1}^{r}\delta(\xi-\xi_i)u_i(t) + \sum_{i=1}^{d}\delta(\xi-\hat{\xi}_i)\tilde{w}_i(t), \tag{79}$$

with boundary conditions

$$\chi(\xi,t)|_{\xi=0,L} = 0, \qquad EI_A\frac{\partial^2\chi(\xi,t)}{\partial\xi^2}\bigg|_{\xi=0,L} = 0,$$

where ρ is the mass per unit length and EI_A is the bending stiffness.

By substituting (54) into (79) and using the orthogonality properties

$$\int_0^L \rho\psi_i(\xi)\psi_j(\xi)d\xi = \delta_{ij}, \qquad \int_0^L EI_A\frac{\partial^4}{\partial\xi^4}\psi_i(\xi)\psi_j(\xi)d\xi = \omega_i^2\delta_{ij},$$

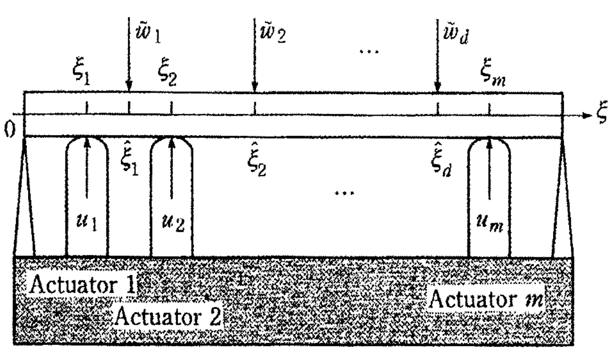

Fig. 10. Simply supported uniform beam.

where δ_{ij} is the Kronecker delta, we obtain (55) with natural frequencies ω_i and eigenfunctions $\psi_i(\xi)$ given by

$$\omega_i = \sqrt{\frac{EI_A}{\rho}}\left(\frac{i\pi}{L}\right)^2, \quad \psi_i(\xi) = \sqrt{\frac{2}{\rho L}}\sin\frac{i\pi\xi}{L}, \quad i = 1, 2, 3, \cdots.$$

For numerical simplicity, let $L = \pi$ and $EI_A = \rho = 2/\pi$ so that

$$\omega_i = i^2, \quad \psi_i(\xi) = \sin i\xi, \quad i = 1, 2, 3, \cdots.$$

Furthermore, two actuators are assumed to be located at $\xi_1 = 1$, $\xi_2 = 2$, and a white noise disturbance with unit intensity is entering at $\hat{\xi}_1 = 1.7$. Finally, we set $\zeta_1 = \zeta_2 = \zeta_3 = 0.01$ and $E_2 = I$ in (16) and retain the first three modes. The resulting energy flows are shown in Fig. 11 for controllers G_{c1}, G_{c2} and G_{c3} designed to maximize $-P_1^c$, $-P_2^c$ and $-P_3^c$, respectively. These results show that each controller maximizes the energy flow from the specified mode and that the energy removed from each subsystem is dissipated by the coupling.

Note that in this example the matrix B of (56) is given by

$$B \triangleq \begin{bmatrix} 0 & 0 \\ 0.8415 & 0.9093 \\ 0 & 0 \\ 0.9093 & -0.7578 \\ 0 & 0 \\ 0.1411 & -0.2794 \end{bmatrix}.$$

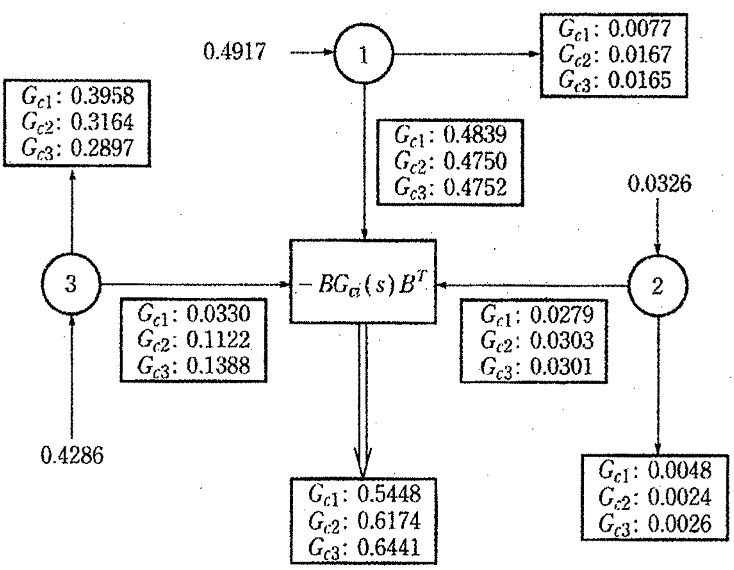

Fig. 11. Energy flow among structural modes with controllers G_{c1}, G_{c2} and G_{c3}.

The elements of the sixth row of B corresponding to the third mode are smaller than the other elements corresponding to the first and the second modes due to the fact that $\xi_1 = 1 \cong L/3$ and $\xi_2 = 2 \cong 2L/3$, that is, actuators 1 and 2 are located near the nodes of the third mode. This suggests, as reflected by Fig. 11, that the controllers are less effective in removing energy flow from the third mode.

Now, we define the steady-state modal energy by

$$\mathscr{E}_i \triangleq \frac{1}{2}\mathscr{E}[\dot{q}_i^2(t)] + \frac{1}{2}\omega_i^2\mathscr{E}[q_i^2(t)], \quad i = 1, 2, 3, \tag{80}$$

and the result is shown in Table 2. Table 2 shows that controller G_{ci} successfully reduces the stored energy $\mathscr{E}_i$ of the ith mode.

Table 2. Steady-state modal energy of the ith mode of a flexible beam

Modal energy	Open-loop	Controller 1	Controller 2	Controller 3
$\mathscr{E}_1$	24.5847	0.3873 (1.58[%])	0.8288 (3.37[%])	0.8276 (3.37[%])
$\mathscr{E}_2$	0.8160	0.0606 (7.43[%])	0.0295 (3.17[%])	0.0482 (5.91[%])
$\mathscr{E}_3$	4.7618	2.1960 (46.12[%])	1.7561 (36.88[%])	1.3266 (27.86[%])

6. Design of an Energy Flow Controller for Relative Force

As a further illustration of the approach of the previous section, we consider the interconnection of two positive real systems $z_i(s)$, $i = 1, 2$, by means of a relative force controller. The controller thus serves as a dissipative coupling as in the previous section. This controller can be viewed as a device for regulating energy flow between two nominally uncoupled subsystems or as an interstitial force device attached to two points on a single structure.

Let $Z^{-1}(s)$ and $G_c(s)$ represent the transfer functions of the two uncoupled strictly positive real systems and the controller, respectively, and assume these systems have the state space realizations

$$\dot{x}_p(t) = Ax_p(t) + B_p u_0(t), \tag{81}$$

$$y_0(t) = C_p x_p(t), \tag{82}$$

$$\dot{x}_c(t) = A_c x_c(t) + B_c y(t), \tag{83}$$

$$u(t) = C_c x_c(t), \tag{84}$$

respectively, where $x_p(t) \in \mathscr{R}^n$, $u(t) \in \mathscr{R}^2$, $x_c(t) \in \mathscr{R}^n$. Now $y_0(t) \in \mathscr{R}^2$ is the velocity vector of the two uncoupled systems and the scalars $y(t)$ and $u(t)$ represent the relative velocity of the subsystems and the relative force applied to each subsystem, respectively.

To obtain the relative velocity $y(t)$ and the coupling force $v_0(t) \in \mathscr{R}^2$ we define $\tilde{B}$ as

$$\tilde{B} \triangleq \begin{bmatrix} 1 \\ -1 \end{bmatrix}, \tag{85}$$

so that $y(t) = \tilde{B}^T y_0(t)$ and $v_0(t) = -\tilde{B}u(t)$. With $\tilde{B}$ given by (85), the feedback system shown in Fig. 12 is equivalent to Fig. 2, where in Fig. 12, $L(s)$ is given by

$$L(s) \triangleq -\tilde{B}G_c(s)\tilde{B}^T. \tag{86}$$

Thus, the coupling $L(s)$ serves as a dissipative controller which controls energy flow between the two subsystems.

Now, (83) and (84) can be rewritten with $\tilde{B}$ as

$$\dot{x}_c(t) = A_c x_c(t) + B_c \tilde{B}^T y_0(t), \tag{87}$$

$$v_0(t) = -\tilde{B}C_c x_c(t), \tag{88}$$

and thus the feedback system (81), (82), (87) and (88) is given by

$$\dot{\tilde{x}}(t) = \tilde{A}\tilde{x}(t) + \tilde{D}\tilde{w}(t), \tag{89}$$

where

$$\tilde{x}(t) \triangleq \begin{bmatrix} x_p(t) \\ x_c(t) \end{bmatrix} \in \mathscr{R}^{2n}, \quad \tilde{A} \triangleq \begin{bmatrix} A & B_p\tilde{B}C_c \\ B_c\tilde{B}^T C_p & A_c \end{bmatrix} \in \mathscr{R}^{2n\times 2n},$$

$$\tilde{D} \triangleq \begin{bmatrix} B_p D \\ B_c D_2 \end{bmatrix} \in \mathscr{R}^{2n\times 2}.$$

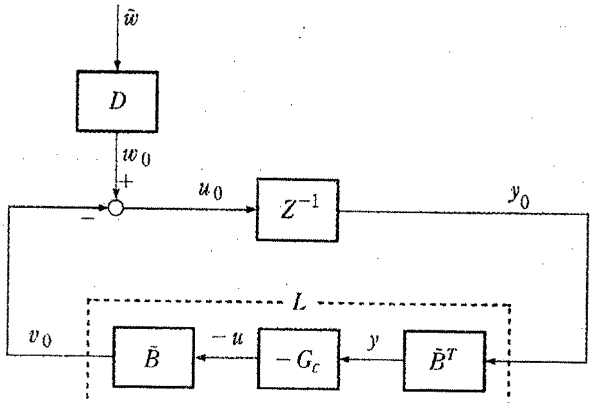

Fig. 12. Feedback representation of coupled system.

By setting $B = B_p\hat{B}$ and $C = \hat{B}^T C_p$, it follows that $\tilde{A} = \begin{bmatrix} A & BC_c \\ B_cC & A_c \end{bmatrix}$ so that (89) has the usual closed-loop structure.

Now we choose the performance variable $E_1 x(t)$ to maximize the energy flow from the ith subsystem, where $i = 1, 2$. By the same argument in the previous sections this is equivalent to minimizing $-P_i^d$.

We now assume that each subsystem $z_i(s)$ has constant real part c_i and define the 2×2 damping matrix C_{d1} by $C_{d1} \triangleq \mathrm{diag}(c_1, c_2)$. Then P_i^d, $i = 1, 2$, is given by

$$P_i^d = -(C_{d1} C_{pa} \tilde{Q} C_{pa}^T)_{(i,i)}, \tag{90}$$

where $C_{pa} \triangleq [C_p \quad 0] \in \mathscr{R}^{2\times 2n}$, and $\tilde{Q}$ satisfies the Lyapunov equation

$$0 = \tilde{A}\tilde{Q} + \tilde{Q}\tilde{A}^T + \tilde{D}\tilde{D}^T. \tag{91}$$

Thus, the performance matrix E_1 in (16) is given by

$$E_1 = \sqrt{c_i}\, e_i^T C_{pa}. \tag{92}$$

Since the plant represented by (A, B, C) is strictly positive real, we can use the positive real control approach to obtain the strictly positive real controller $-G_c(s)$.

To illustrate this approach we consider the two oscillator system with coupling $L(s)$ shown in Fig. 13, where f represents the relative force. For illustrative purposes we set $k_1 = 10$, $k_2 = 2$, $m_1 = 0.3$, $m_2 = 0.4$ and $c_1 = 0.1$, $c_2 = 0.2$, and let the white noise disturbances $w_i(t)$, $i = 1, 2$, have unit intensity, that is, $D = I$. By setting $E_2 = 0.1$ in (16) we design the controllers G_{c1} and G_{c2} to maximize $-P_1^c$ and $-P_2^c$, respectively. The resulting energy flows given in Fig. 14 show that each controller successfully removes energy from the specified subsystem by minimizing the dissipated energy flow out of the subsystem. The steady-state stored energy $\mathscr{E}_i$, $i = 1, 2$, defined by (53) is listed in Table 3, which shows that each controller successfully reduces the stored energy of the corresponding oscillator. Finally, the Bode plots of the controllers in Fig. 15 show that the controllers are strictly positive real.

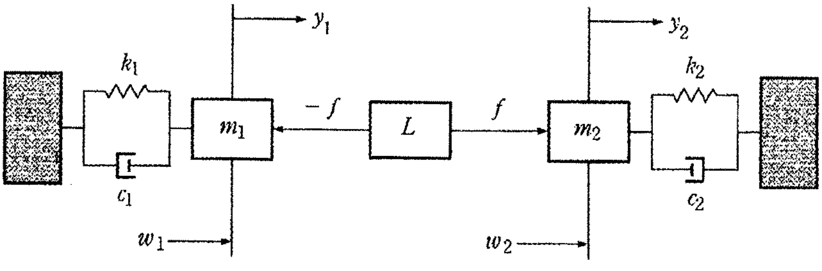

Fig. 13. Two oscillator system with relative force controller coupling.

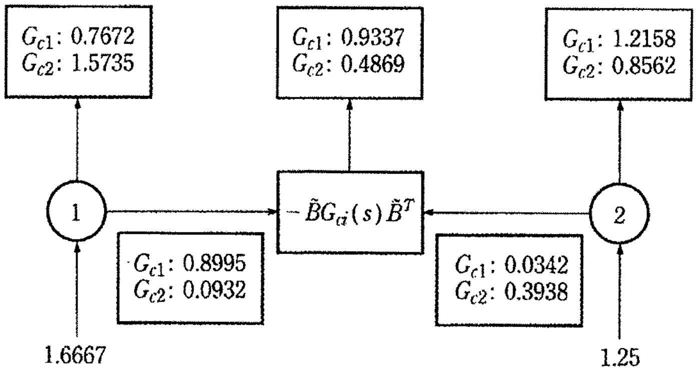

Fig. 14. Energy flow between oscillators with controllers G_{c1} and G_{c2}.

Table 3. Steady-state stored energy for two coupled oscillators with relative force actuator

Stored energy	Open-loop	Controller 1	Controller 2
$\mathscr{E}_1$	5.0	2.6401 (52.08[%])	4.5683 (91.37[%])
$\mathscr{E}_2$	2.5	2.3549 (94.20[%])	1.2041 (48.16[%])

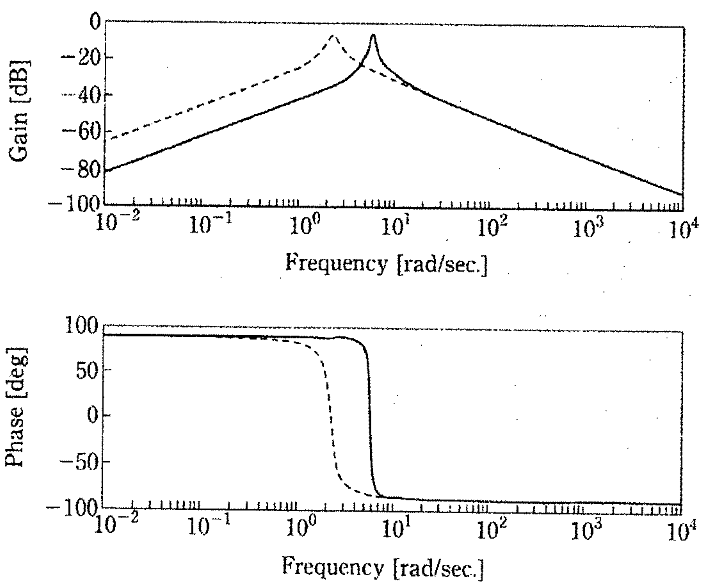

Fig. 15. Magnitude and phase of controllers G_{c1} (solid) and G_{c2} (dashed).

7. Conclusion

In this paper, we applied energy flow models obtained in Kishimoto and Bernstein (1995 a; b), Kishimoto et al. (1995 a) and Wyatt et al. (1984) to design energy flow controllers for modal subsystems. By using the LQG positive real control approach, each controller was considered as either an additional subsystem or as a dissipative coupling. Each resulting controller was shown to maximize energy flow from the specified subsystem. Furthermore, closed-loop asymptotic stability is guaranteed since strictly positive real controllers were designed in a negative feedback loop. These features were demonstrated by numerical examples.

References

Anderson, B.D.O. and S. Vongpanitlerd (1973). *Network Analysis and Synthesis: A Modern Systems Theory Approach*. Prentice-Hall, Englewood Cliffs, N.J.

Benhabib, R.J., R.P. Iwens and R.L. Jackson (1981). Stability of large structure control systems using positivity concepts. *J. Guid. Contr.*, **4**, 487–494.

Bernstein, D.S. and D.C. Hyland (1991). Compartmental analysis and power flow analysis for state space systems. S.P. Bhattacharyya and L.H. Keel (eds.), *Control of Uncertain Dynamic Systems*, CRC Press, Boca Raton, FL, 175–202.

Boyd, S.P. and C.H. Barratt (1991). *Linear Controller Design*. Prentice-Hall, Englewood Cliffs, N.J.

Crandall, S.H. and R. Lotz (1971). On the coupling loss factor in statistical energy analysis. *J. Acoust. Soc. Amer.*, **49**, 352–356.

Davies, H.G. (1972 a). Exact solutions for the response of some coupled multimodal systems. *J. Acoust. Soc. Amer.*, **51**, 387–392.

Davies, H.G. (1972 b). Power flow between two coupled beams. *J. Acoust. Soc. Amer.*, **51**, 393–401.

Davies, H.G. (1973). Random vibration of distributed systems strongly coupled at discrete points. *J. Acoust. Soc. Amer.*, **54**, 507–515.

Haddad, W.M., D.S. Bernstein and Y.W. Wang (1994). Dissipative H_2/H_∞ control synthesis. *IEEE Trans. Automatic Control*, **AC-39**, 827–831.

Kishimoto, Y. and D.S. Bernstein (1995 a). Thermodynamic modeling of interconnected systems: I. Conservative coupling. *J. Sound Vib.*, **182**, 23–58.

Kishimoto, Y. and D.S. Bernstein (1995 b). Thermodynamic modeling of interconnected systems: II. Dissipative coupling. *J. Sound Vib.*, **182**, 59–76.

Kishimoto, Y., D.S. Bernstein and S.R. Hall (1995 a). Energy flow modeling of interconnected systems: A deterministic foundation for statistical energy analysis. *J. Sound Vib.*, **186** (to appear).

Kishimoto, Y., D.S. Bernstein and S.R. Hall (1995 b). Energy flow control of interconnected structures: II. Structural subsystems. *Control–Theory and Advanced Technology (C-TAT)*, **10**, 4, Part 4, 1591–1618.

Langley, R.S. (1992). A wave intensity technique for the analysis of high frequency vibration. *J. Sound Vib.*, **159**, 483–502.

Lozano-Leal, R. and S.M. Joshi (1990). On the design of dissipative LQG-type controllers. *Proc. IEEE Conference on Dec. Contr.*, Honolulu, 3492–3495.

Lyon, R.H. (1975). *Statistical Energy Analysis of Dynamical Systems: Theory and Applications*. MIT Press, Cambridge, MA.

Lyon, R.H. (1987). *Machinery Noise and Diagnostics*. Butterworth, Boston.

Lyon, R.H. and G. Maidanik (1962). Power flow between linear coupled oscillators. *J. Acoust. Soc. Amer.*, **34**, 623–639.

Mace, B.R. (1987). Active control of flexural vibrations. *J. Sound Vib.*, **114**, 253–270.

Mace, B.R. (1992 a). Power flow between two continuous one-dimensional subsystems: A wave solution. *J. Sound Vib.*, **154**, 289–320.

Mace, B.R. (1992 b). Power flow between two coupled beams. *J. Sound Vib.*, **159**, 305–327.

MacMartin, D.G. and S.R. Hall (1991). Control of uncertain structures using an H_∞ power flow approach. *J. Guidance, Control, and Dynamics*, **14**, 521–530.

MacMartin, D.G. and S.R. Hall (1994). Broadband control of flexible structures using statistical energy analysis concepts. *J. Guidance, Control, and Dynamics*, **17**, 361–369.

Maidanik, G. (1981). Extension and reformulation of statistical energy analysis with use of room acoustics concepts. *J. Sound Vib.*, **78**, 417–423.

Miller, D.W. and A.H. Von Flotow (1989). Power flow in structural networks. *J. Sound Vib.*, **12**, 145–162.

Miller, D.W., S.R. Hall and A.H. Von Flotow (1990). Optimal control of power flow at structural junctions. *J. Sound Vib.*, **140**, 475–497.

Newland, D.E. (1968). Calculation of power flow between coupled oscillators. *J. Sound Vib.*, **3**, 553–559.

Norton, M.P. (1989). *Foundations of Noise and Vibration Analysis for Engineers*. Cambridge University Press, Cambridge.

Pan, J. and C.H. Hansen (1991). Active control of total vibratory power flow in a beam. I: Physical system analysis. *J. Acoust. Soc. Amer.*, **89**, 200–209.

Pan, J., J. Pan and C.H. Hansen (1992). Total power flow from a vibrating rigid body to a thin panel through multiple elastic mounts. *J. Acoust. Soc. Amer.*, **92**, 895–907.

Pinnington, R.J. and R.G. White (1981). Power flow through machine isolators to resonant and non-resonant beams. *J. Sound Vib.*, **75**, 179–197.

Smith, Jr., P.W. (1979). Statistical models of coupled dynamical systems and the transition from weak to strong coupling. *J. Acoust. Soc. Amer.*, **65**, 695–698.

Von Flotow, A.H. (1986). Disturbance propagation in structural networks. *J. Sound Vib.*, **106**, 433–450.

Von Flotow, A.H. and B. Shäfer (1986). Wave-absorbing controllers for a flexible beam. *J. Guidance, Control, and Dynamics*, **9**, 673–680.

Wyatt, J.L., W.M. Siebert and H.N. Tan (1984). A Frequency Domain Inequality for Stochastic Power Flow in Linear Networks. *IEEE Trans. Circuits and Systems*, **31**, 809–814.

Woodhouse, J. (1981). An approach to the theoretical background of statistical energy analysis applied to structural vibration. *J. Acoust. Soc. Amer.*, **69**, 1695–1709.

Yasuo Kishimoto was born in Kobe, Japan in 1961. He received the B.S. and M.S. degrees in aeronautical engineering from the National Defense Academy, Yokosuka, Japan, in 1985 and 1990, respectively. He received the Ph.D. degree in aerospace engineering in 1993 from the University of Michigan. Since 1985, he has been an officer in the Japan Air Self Defense Force. His research interests include energy flow modeling and control for interconnected structures.

Dennis S. Bernstein is an Associate Professor in the Department of Aerospace Engineering at The University of Michigan in Ann Arbor, Michigan. From 1982–84, he was employed by MIT Lincoln Laboratory, and from 1984 to 1991, he worked for Harris Corporation in Melbourne, Florida.

At the University of Michigan he has taught courses on control of flexible structures and multivariable feedback control theory. His theoretical research interests include both linear control (fixed-structure control, robust control, and sampled-data control) and nonlinear control (Hamilton-Jacobi theory, saturating control and absolute stability). Applied areas of interest include control of vibrations, acoustics and fluids with application to flexible structures, noise suppression, and slosh, as well as control of rigid body motion with application to rotating spacecraft and unbalanced rotating machinery.

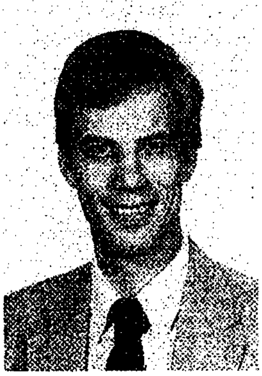

Steven R. Hall received his S.B., S.M. and Sc.D. degrees from the Massachusetts Institute of Technology Department of Aeronautics and Astronautics in 1980, 1982 and 1985, respectively. Since 1985, he has been on the faculty of the Massachusetts Institute of Technology, where he is Associate Professor of Aeronautics and Astronautics. His research interests include active control of flexible structures and the control of helicopter vibration and rotor dynamics. He is an Associate Fellow of the AIAA and a member of the IEEE and the American Helicopter Society. He is also a member of the AIAA Guidance, Navigation and Control Technical Committee.